Cell Reports Medicine, Volume *4*

Supplemental information

Potential therapeutic implications of histidine catabolism by the gut microbiota in NAFLD patients with morbid obesity

Sergio Quesada-Vázquez, Anna Castells-Nobau, Jèssica Latorre, Núria Oliveras-Cañellas, Irene Puig-Parnau, Noemi Tejera, Yaiza Tobajas, Julio Baudin, Falk Hildebrand, Naiara Beraza, Rémy Burcelin, Laura Martinez-Gili, Julien Chilloux, Marc-Emmanuel Dumas, Massimo Federici, Lesley Hoyles, Antoni Caimari, Josep M. del Bas, Xavier Escoté, José-Manuel Fernández-Real, and Jordi Mayneris-Perxachs

a

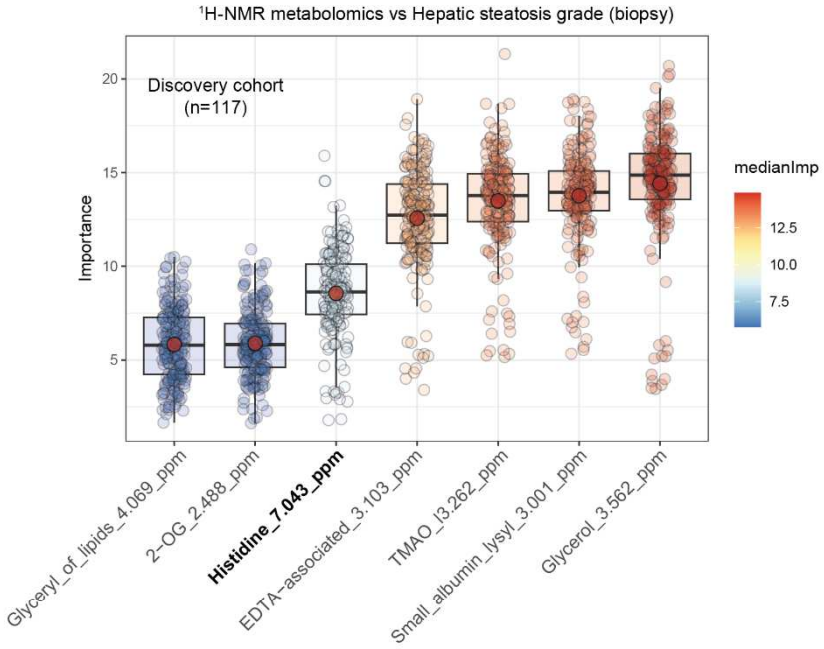
¹H-NMR metabolomics vs Hepatic steatosis grade (biopsy)
Discovery cohort
(n=117)
Importance
medianImp
12.5
10.0
7.5
Glyceryl_of_lipids_4.069_ppm
2-OG_2.488_ppm
Histidine_7.043_ppm
EDTA-associated_3.103_ppm
TMAO_3.262_ppm
Small_albumin_lysyl_3.001_ppm
Glycerol_3.562_ppm

b

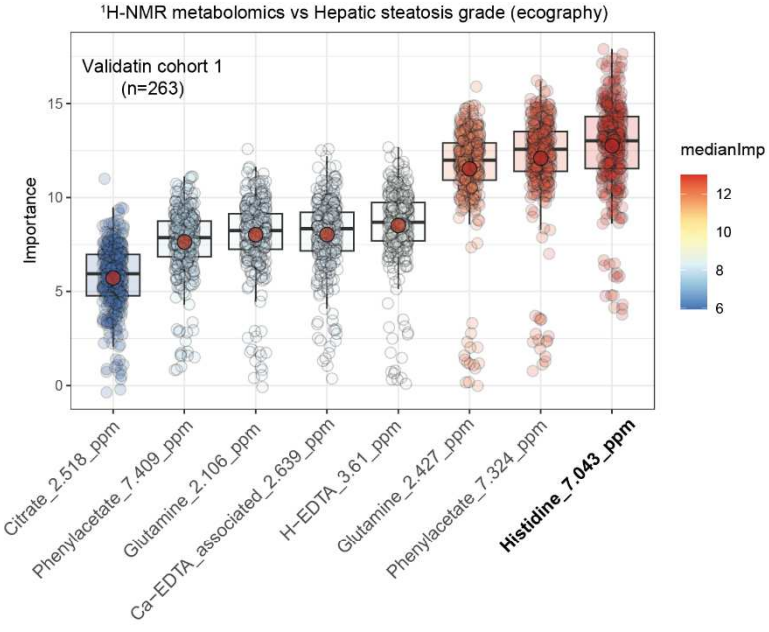
¹H-NMR metabolomics vs Hepatic steatosis grade (ecography)
Validatin cohort 1
(n=263)
Importance
medianImp
12
10
8
6
Citrate_2.518_ppm
Phenylacetate_7.409_ppm
Glutamine_2.106_ppm
Ca-EDTA_associated_2.639_ppm
H-EDTA_3.61_ppm
Glutamine_2.427_ppm
Phenylacetate_7.324_ppm
Histidine_7.043_ppm

c

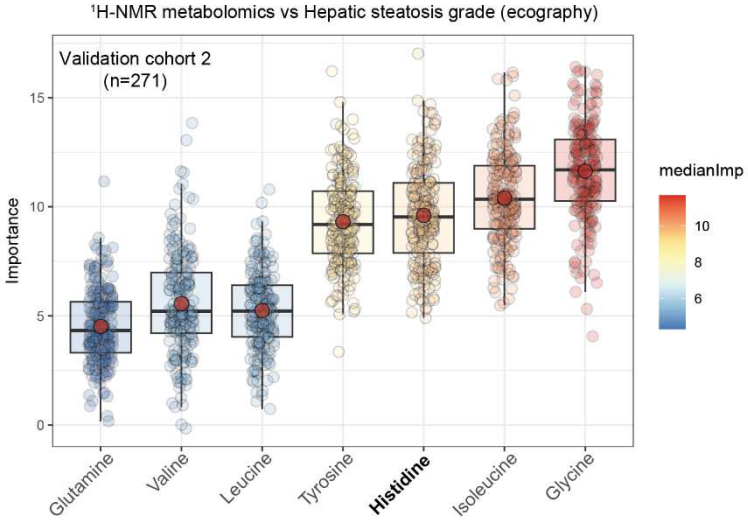
¹H-NMR metabolomics vs Hepatic steatosis grade (ecography)
Validation cohort 2
(n=271)
Importance
medianImp
10
8
6
Glutamine
Valine
Leucine
Tyrosine
Histidine
Isoleucine
Glycine

Figure S1. Associations of the plasma histidine metabolome with the steatosis grade. a-c) Boxplots of the normalized permutated variable importance measure (VIM) for the metabolites associated with the liver steatosis grade after controlling for age, BMI, gender, country, and fasting glucose levels, in the Discovery cohort (n = 117, biopsy), the Validation cohort 1 (n = 263, echography), and the Validation cohort 2 (n = 271, echography), respectively. Metabolites were identified using the random-forest based machine learning variable selection algorithm Boruta using 2000 trees, 500 iterations, and P-Bonferroni < 0.005. Related to Figure 1.

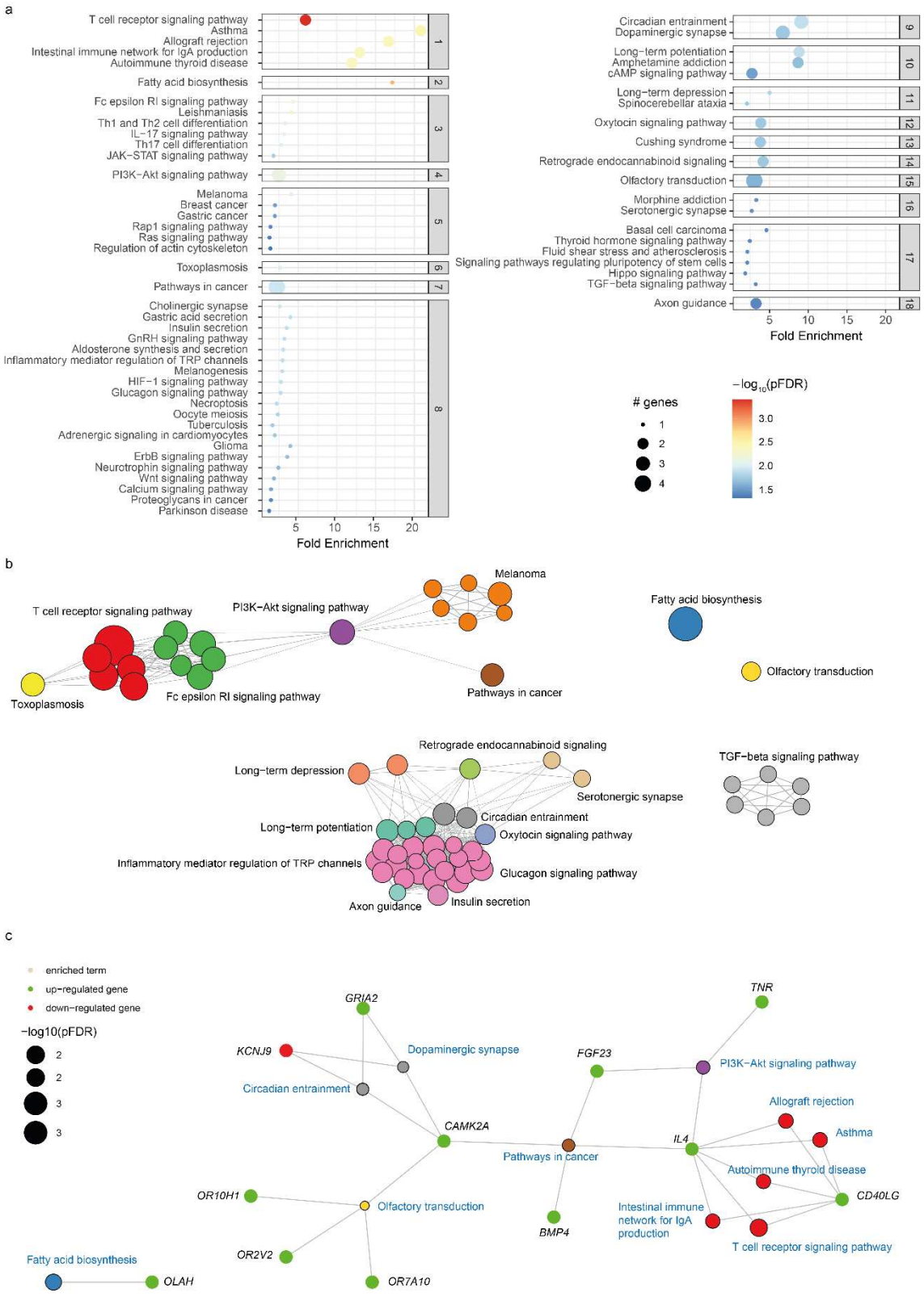

Figure S2. Associations of the liver transcriptome gene expression with the circulating histidine levels. a) Dot plot of KEGG-based over-representation analysis results performed on active subnetworks grouped by hierarchical clustering. The *x*- axis represents the fold enrichment defined as the ratio of the frequency of input genes annotated in a pathway to the frequency of all genes annotated to that pathway.

The dot size indicates the number of differentially expressed genes in a given pathway. Dots are coloured by the -$\log_{10}$(pFDR), with red indicating higher significance. **b)** Enrichment map inter-related significant pathways identified using an active subnetwork- oriented approach. Each colour displays a cluster of related pathways using a threshold for kappa statistics = 0.35. The size of the nodes corresponds to its -$\log_{10}$(pFDR). The thickness of the edges between nodes corresponds to the kappa statistic between the two nodes. **c)** Gene-concept network depicting significant genes involved in enriched pathways from selected clusters. The dot size of the pathways represents the -$\log_{10}$(pFDR). Pathways with the same colour correspond to the same cluster. Related to Figure 2.

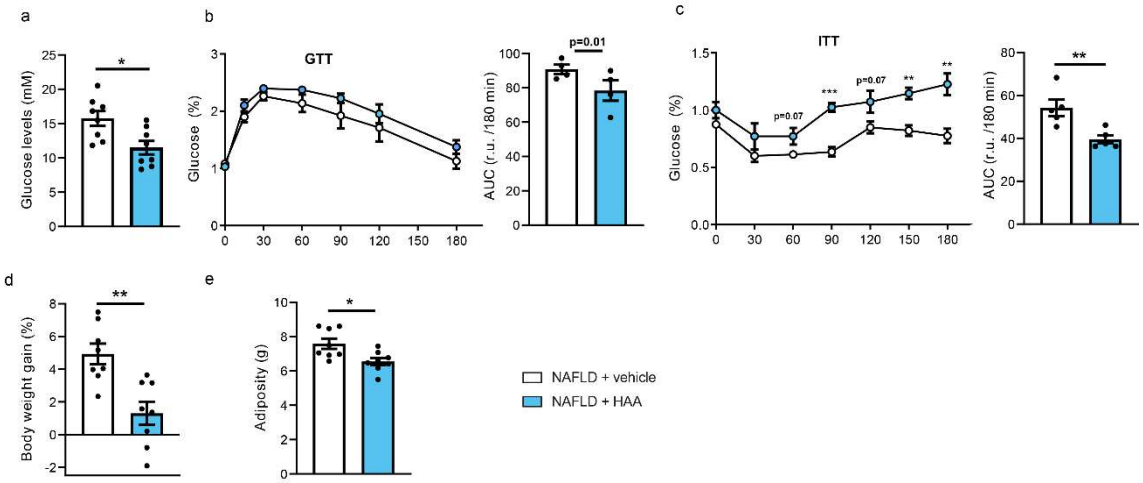

Figure S3. **Effects of HAA supplementation in glucose metabolism and adiposity. a)** Fasting glucose; **b)** glucose tolerance test (GTT) and area under the curve (AUC); **c)** insulin tolerance test (ITT) and AUC; **d)** Body weight gain; **e)** Adiposity Data are mean ± SEM. * $P < 0.05$, ** $P < 0.01$, *** $P < 0.001$. Related to Figure 3.

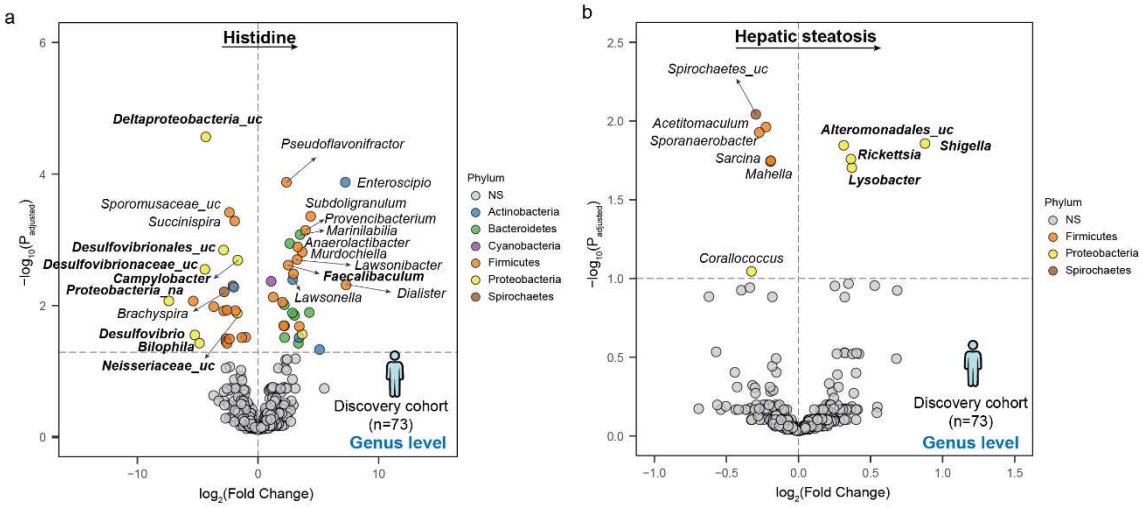

Figure S4. **Associations of plasma histidine and steatosis degree with the gut microbiota at the genus level.** Volcano plot of differential bacteria genera associated with **a)** the circulating histidine levels and **b)** hepatic steatosis in the discovery cohort (*n*=73) identified using the Analysis of Microbiomes with Bias Correction (ANCOM-BC) controlling for age, BMI, gender, and country. The $\log_2$(Fold Change) associated with a unit change in the plasma histidine levels and the -$\log_{10}$(p-values) adjusted for multiple testing are plotted for each genus. Related to Figure 5.

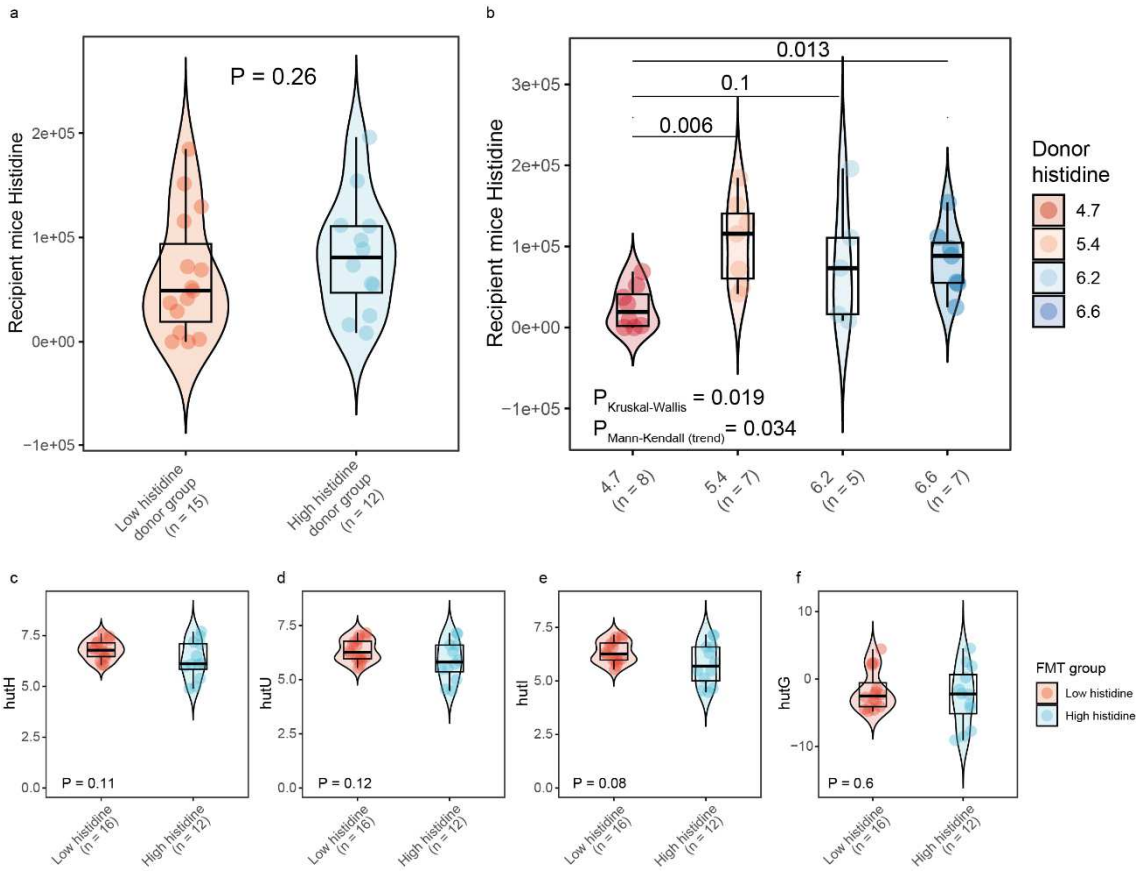

Figure S5. **Histidine and histidine utilization system microbial molecular function in recipient mice.** **a)** Plasma histidine levels in the recipient mice receiving microbiota from donors with low histidine levels (below the median) and high histidine levels (above the median). **b)** Plasma histidine levels in recipient mice according to the circulating histidine levels of the donor. **c-f)** Violin plots of the centered log ratio-transformed predicted microbial genes involved in histidine utilisation *hutH, hutU, hutI* and *hutG*, respectively, in mice receiving microbiota from donors with low histidine and high histidine levels. Related to Figure 6.